FEBS Letters 588 (2014) 1230–1237

journal homepage: www.FEBSLetters.org

Review

Structure and closure of connexin gap junction channels

Atsunori Oshima *

Cellular and Structural Physiology Institute (CeSPI), Nagoya University, Furo-cho, Chikusa-ku, Nagoya 464-8601, Japan
Department of Basic Medicinal Sciences, Graduate School of Pharmaceutical Sciences, Nagoya University, Furo-cho, Chikusa-ku, Nagoya 464-8601, Japan

ARTICLE INFO

Article history:
Received 28 November 2013
Revised 24 January 2014
Accepted 24 January 2014
Available online 1 February 2014

Edited by Michael Koval, Brant E. Isakson, Robert G. Gourdie and Wilhelm Just

Keywords:
Connexin
Structure
Function
Gating
Electron microscopy
X-ray crystallography

ABSTRACT

Connexin gap junctions comprise assembled channels penetrating two plasma membranes for which gating regulation is associated with a variety of factors, including voltage, pH, Ca^{2+}, and phosphorylation. Functional studies have established that various parts of the connexin peptides are related to channel closure and electrophysiology studies have provided several working models for channel gating. The corresponding structural models supporting these findings, however, are not sufficient because only small numbers of closed connexin structures have been reported. To fully understand the gating mechanisms, the channels should be visualized in both the open and closed states. Electron crystallography and X-ray crystallography studies recently revealed three-dimensional structures of connexin channels in a couple of states in which the main difference is the conformation of the N-terminal domain, which have helped to clarify the structure in regard to channel closure. Here the closure models for connexin gap junction channels inferred from structural and functional studies are described in the context of each domain of the connexin protein associated with gating modulation.

1. Introduction

Most multicellular organisms have established intercellular communication mediated by gap junctions. These junctions comprise assemblies of channels in which two hemichannels are docked head-to-head with each other, and a patch of channel clusters is referred to as a gap junction plaque. The term "gap" refers to the narrow clearance of 2–4 nm between the two adjoining cells [1]. The central pore of the channel allows for the transfer of small signaling molecules with relatively low specificity, and the adjacent cells are coupled together electrically as well as chemically.

Genetic studies have revealed that the molecular component of vertebrate gap junction channels is connexin (Cx) [2–4], which contains four-pass transmembrane domains (TM1–TM4), two extracellular loops (EL1, EL2), cytoplasmic N- and C-terminal domains (NT, CT), and a single cytoplasmic loop (CL). Over 20 members of the connexin family with the same topology have been identified, and these differ mainly in the lengths and sequences of cytoplasmic loop (CL) and carboxyl terminal domain (CT) [5]. Because gap junction channels autonomously form channel clusters, and sometimes a two-dimensional (2D) crystal lattice, great effort has been devoted to developing an isolation protocol for rodent liver gap junctions [6–10], and electron microscopy (EM) and X-ray diffraction studies performed in the 1970s led to a dodecameric connexin model of the gap junction structure [11].

Along with these structural studies, functional electrophysiology and dye permeability studies determined that cytoplasmic pH and calcium ions modulate gap junction channel activity [12–14]. Around the same time, electrophysiology findings revealed that junctional voltage regulates the intercellular coupling of connexin channels [15], and a model with charge-sensing residues lying within an aqueous pore was proposed [16]. It is now accepted that connexin channel activities are also modulated by various chemical factors, such as amino sulfonates, phosphorylation, lipophiles, cyclic nucleotides, and others [17]. Comprehensive structural models that rationally account for the conformational changes corresponding to these gating modifications, however, are currently insufficient. Traditional and recent structural studies are reviewed here along with the gating movements inferred from functional studies.

2. Three-dimensional structures of connexin gap junction channels; historical overview

The first three-dimensional (3D) reconstruction of connexin was generated by electron crystallography with negatively-stained

Abbreviations: Cx, connexin; Vj, transjunctional voltage; NT, amino terminal domain; CT, carboxyl terminal domain; CL, cytoplasmic loop; EL, extracellular loop; TM, transmembrane helix; EM, electron microscopy; Cx32*Cx43E1, Cx32 chimera in which the EL1 of Cx32 is replaced with the EL1 of Cx43; MD, molecular dynamics

* Corresponding author at: Cellular and Structural Physiology Institute (CeSPI), Nagoya University, Furo-cho, Chikusa-ku, Nagoya 464-8601, Japan. Fax: +81 52 747 6795.
E-mail address: atsu@cespi.nagoya-u.ac.jp

http://dx.doi.org/10.1016/j.febslet.2014.01.042
0014-5793/

rat liver gap junctions [18] and cryo EM [19], providing a model for open and closed rearrangement by tilting the subunits in response to the Ca^{2+} concentration [19,20]. This model, referred to as the subunit rotation model, is based on the high degree of cooperativity between subunits (Fig. 1(A)) [21]. First, at least all six subunits in a hemichannel (connexon) simultaneously assume an identical conformational change in a concerted manner. Second, although rearrangement of the subunits in one hemichannel tangential to the channel centers around the extracellular docking surface, the allosteric conformational change of the apposed hemichannel is not negligible. Therefore, it is thought that two docked hemichannels move in conjunction with each other. Structural studies with isolated native gap junctions, followed by EM for split gap junctions in a cryo-negative preparation, revealed six protrusions on the extracellular surface [22]. After recombinant expression of connexin in cultured mammalian cells was established [23,24], electron crystallography revealed a 3D structure of a truncated Cx43 mutant at 7.5 Å resolution [25]. While this structure clearly demonstrated 24 transmembrane helices, thereby validating the models of hexameric hemichannels and dodecameric junction channels, it was unclear whether the channel was open or closed because of the wide pore pathway despite the addition of oleamide, a potential blocker for gap junction channels [26], to the crystallization buffer.

The gap junction structure in an obviously closed state was derived from 2D crystals of Cx26 with a single point mutation from Met to Ala at position 34 (Cx26M34A) [27,28]. This mutant is a derivative of the hereditary hearing-loss mutant M34T [29], and its permeability to dye tracer is significantly decreased, if not completely blocked, indicating that it favors a closed state [30]. The 3D structure of Cx26M34A reconstructed at 10 Å resolution (a vertical resolution of 14 Å) revealed an aggregate density, termed a plug, in

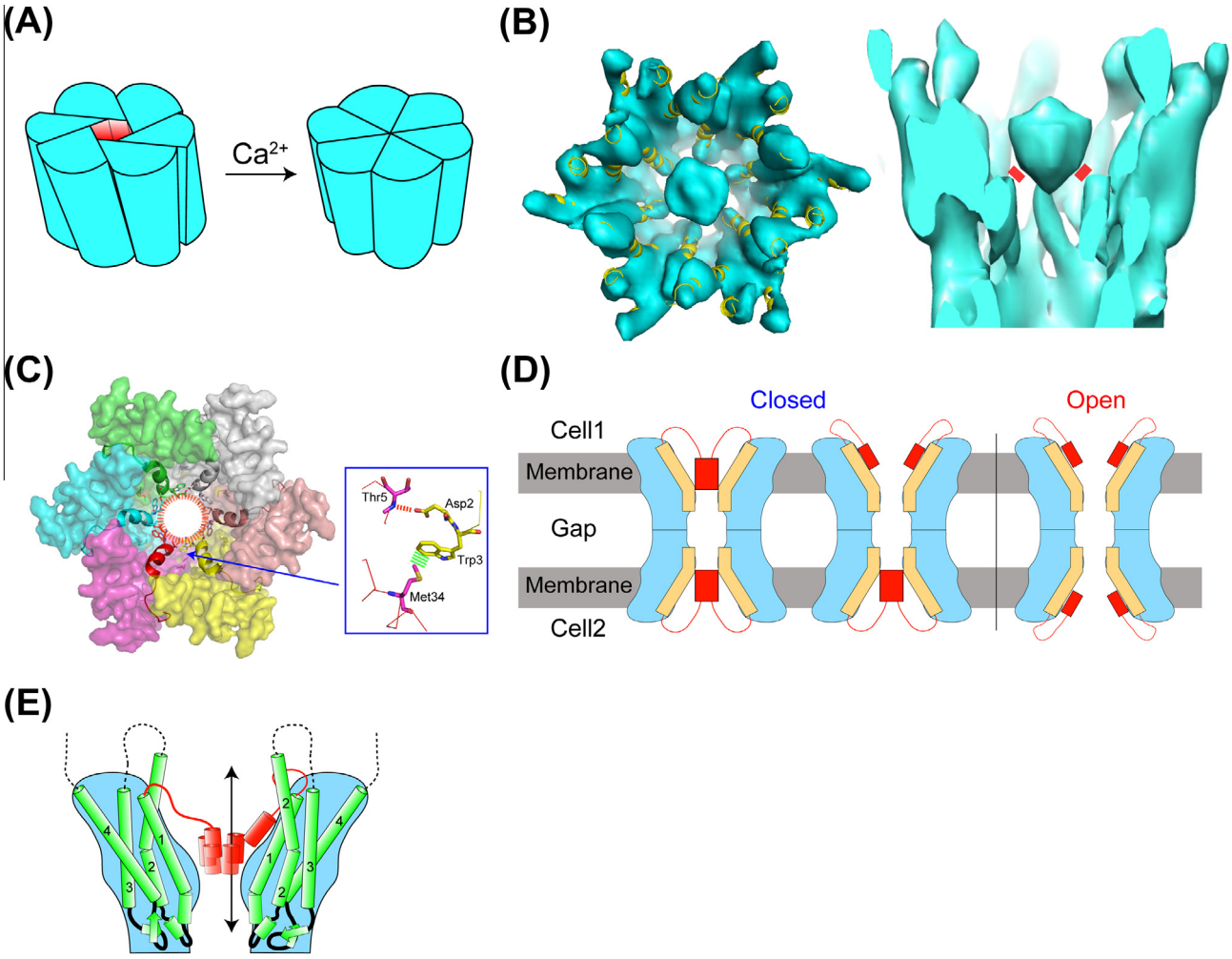

Fig. 1. Gating models inferred from structural studies of connexin gap junction channels. (A) Subunit rotation model [19]. Ca^{2+} induces the gating transitions of the gap junction channel between open and closed configurations. Tilted subunits in a hemichannel assume a tangential displacement upon exposure to Ca^{2+}. The subunits move inward and narrow the pore near the cytoplasmic membrane surface. (B) 3D structure of a Cx26M34A mutant corresponding to a hemichannel portion in a surface representation contoured at 1.0σ reconstructed by electron crystallography [27]. (left) Top view shows the density in the vestibule plugging the pore pathway. The helix ribbon model is shown next to the Cx26 X-ray structure (PDB code: 2ZW3) [32], fitted into the EM map where the NT portions are eliminated for a different conformation. (right) Side view reveals that the constriction between the plug and TM1 is less than 6 Å (shaded in red), which would not permit any transfer of hydrated ions. (C) Top view of Cx26 X-ray structure [32] demonstrates the N-terminal arrangements in an open conformation. The six NT helices form a pore funnel stabilized by a circular network of hydrogen bonds (broken circle in orange). The residues relevant to the interactions for the funnel formation are shown in stick model. (Inset) Detailed representation of the interactions that stabilize the pore funnel, which involve the hydrogen bond between Asp2 and Trp5 (orange dotted line) and the hydrophobic interaction between Trp3 and Met34 (green dotted line). (D) Schematic representation of hypothesized plug gating mechanism of gap junctions. Each hemichannel (cyan) has its own plug formed by an assembly of NTs, and can regulate its channel activity autonomously. The gap junction is open only when the N-termini (red) in both hemichannels assume an open conformation (modified from [27] and [32]). (E) For hydrated ion permeation of the plug-gated structure, the movement of one N-terminal helix would be sufficient to create an 8 Å space to pass through.

the pore vestibule of each hemichannel, demonstrating a closed state of Cx26 (Fig. 1(B)) [27]. This structure, however, did not resolve the part of the connexin peptide that corresponds to the plug due to limited resolution. The N-terminal deletion mutant, Cx26M34Adel2-7, was also crystallized in 2D, and the projection map revealed a significant decrease in the plug density, indicating that the N-terminal portion of Cx26 forms the plug [31], which was supported by a 3D reconstruction of Cx26M34Adel2-7 [28]. A major breakthrough in high-resolution structural studies of gap junction channels was achieved by the X-ray crystal structure of Cx26 at 3.5 Å resolution, which was considered to be in an open conformation because the structure, in contrast to the EM structure of Cx26M34A, showed no hindrance in the pore vestibule [32]. The molecular dimensions of the Cx26 X-ray structure are similar to earlier EM structures. The external channel diameter, which is largest at the end of the cytoplasmic end, is ~90 Å, the channel height normal to the membrane is ~155 Å, and the extracellular gap width is 40 Å [32]. Although most of the CL and CT is disordered, resulting in ambiguity in those regions, this structure clarified several unknowns, such as the helical arrangement in the membranes, the docking surface interactions of the apposed hemichannels, and the arrangements between adjacent subunits in a single hemichannel, the details of which are described elsewhere [33]. In this review, I focus specifically on the NTs that form the pore constriction in the latest EM and X-ray structures of Cx26 in connection with current findings from electrophysiology studies.

3. Closed state and plug-gating models for connexin gap junction channels

A prominent feature represented by the X-ray structure of Cx26 is the amino terminal domain (NT) portion located in the pore vestibule. The six N-termini make up the conformation of the short α-helix, which is consistent with the nuclear magnetic resonance (NMR) solution structures of Cx26, Cx37, and Cx43 NT peptides [34–36], forming a pore funnel that supports the open conformation of the channel by creating a hydrogen bond network through Asp2 and Thr5, like a circular girdle (Fig. 1(C)) [32]. The N-terminal pore funnel constricts the channel pore with a diameter of ~14 Å near the extracellular membrane surface, and thus this structure suggests that the plug observed in the EM structure of Cx26M34A comprises an assembly of NTs. In addition, the pore funnel is stabilized underneath by hydrophobic interactions with the side chain of Met34 (Fig. 1(C)), in accordance with the generation of the plug density in the Cx26M34A mutant where the short side chain of Ala34 would be too far (>5 Å) from Trp3 to form hydrophobic interactions to support the pore funnel, resulting in a collapse of the hydrogen bond network and thus to channel closure by the NT aggregate [32,33]. Although the cytoplasmic domains, most of which are still unresolved in both EM and X-ray structures, should be considered, these structures support the notion that the NTs are associated with closure as an entity of a certain gate present in the gap junction channel. The general idea behind the plug-gating model is that closure of the connexin gap junction channel is mediated by the physical N-terminal blockage in the vestibule, and the apposed hemichannels can regulate their gating independently (Fig. 1(D)).

The most difficult problem to overcome in structural studies of the gating mechanism of gap junction channels is the absence of a recognizable structure of wild-type connexin in a closed state at mid-to-high resolution. It might be very difficult to fix wild-type connexin channels in a closed state under general crystallization conditions because most reported 3D reconstructions of gap junction channels and hemichannels show a wide pore, as if they are open [18,19,22,25,32,37,38]. Even the structure considered to be in a closed state induced by subunit rotation in response to Ca^{2+} has a pore diameter of up to more than 15 Å [19], which would likely allow for the transfer of hydrated ions if there is no other hindrance. Two models, however, might represent an identifiable closed conformation. One results from atomic force microscopy imaging studies that elucidated the conformational change induced by Ca^{2+} using the hemichannel membranes where the undocked extracellular entrance of the pore is dynamically and reversibly modulated to be narrow, although the change at the cytoplasmic surface is still ambiguous due to the low resolution [39]. This extracellular rearrangement may be distinct from that which occurs in the junction form because of the tightly sealed interactions that are mediated mainly by hydrogen bonds between the ELs of apposed hemichannels [32], and also because another atomic force microscopy study reported that the extracellular domains of reconstituted undocked hemichannels are structurally different from those separated by the docked gap junctional plaques [40]. The other model is the EM structure of Cx26M34A, which is currently the only structure of a junction form in a closed state at a resolution that shows features of the transmembrane helices. It should be noted, however, that the Cx26M34A structure with a physical blockage in the pore vestibule is from a mutant Cx26 construct, and thus may not represent functional or physiologic closure. The similarity of the plug-gated structure with functional movement in the context of various gating mechanisms demonstrated by functional studies, therefore, remains unknown.

The functional properties of Cx26M34A have been investigated using a fluorescent dye transfer assay and recording electrical conductance. The dye permeability of the Cx26M34A gap junction channel is significantly decreased, but a little higher than background [30], indicating that this channel is not fully impermeable. Single channel recordings also support the active function of this mutant, showing the Cx26M34A hemichannels with a narrow range of conductance as compared with wild-type Cx26 [41]. In paired *Xenopus* oocyte experiments, while Cx26M34A fails to induce measurable intercellular conductance in homotypic pairings, heterotypic pairings of the mutant with wild-type Cx26 still exhibit functionality, albeit with 90% reduced conductance, and normal voltage gating (Vj-gating; described below) current decay was observed [28]. These findings suggest that the Cx26M34A mutant is still functional, but favors a closed state induced by a decreased open probability. A simple interpretation is that the plug-gated EM structure comprising homo dodecameric Cx26M34A peptides represents a fully closed architecture because the constriction forms a pore as narrow as 6 Å, which is not large enough for hydrated ions to permeate (Fig. 1(B)) [27]. The first thought of a plug-gating model was undoubtedly inspired by the concept of Vj-gating, but the plug-gated structure may not correlate with the Vj-gated conformation because no voltage is applied to the 2D crystals of Cx26M34A and the Vj-gating property does not allow for the fully closed conformation [42,43]. At present, the opening mechanism of Cx26M34A that allows for small conductivity when making a heterotypic pairing with the wild-type peptide is still unclear. For the permeation of hydrated ions, channel constriction must be widened to more than 8 Å in diameter, which requires a conformational change and/or positional rearrangement of the plug structure, such as by drawing at least one N-terminal helix away from a plug (Fig. 1(E)). Given the positive activity of Cx26M34A mutant channels, the plug would not be locked but would maintain some mobility in the vestibule. This is also accounted for by the observation that the orientation of the side chain of some residues in the connecting N-terminal loop, which was mostly disordered in the EM structures [27,28], is not precisely defined because of the poor electron density with a B-factor as high as ~200 $Å^2$ in the X-ray structure [32]. It is clear, however, that the plug-gated structure depicts a closed state, i.e., one closed state among many potential models, in that the physical blockage in

the pore decreases the functionality of Cx26 gap junction channels in terms of permeability and electrical activity.

4. Vj-gating and individual subunit model

It is well established that connexin NTs are associated with the gating mechanism of gap junction channels in response to Vj, called Vj-gating (fast-gating) [44]. Vj-gating exhibits gating transitions within several milliseconds to a stable subconducting state, described as the residual conductance state, in which the pore is not fully occluded to ion conduction [42,43]. The Vj-dependent property is intrinsic to the hemichannel, suggesting that each hemichannel has its own gate that responds to transjunctional voltage (Vj) [16]. This concept is well reconciled with the Cx26M34A structure if the plug functions as a gate that allows for independent movement between the docked hemichannels. The connexin NTs are essential for determining the gating polarity serving as a Vj sensor [44]. The NTs, specifically the first 10 amino acids, are located in the pore entrance to sense the voltage field, based on the fact that the gating polarity of Vj-gating is reversed by single amino acid mutations in the NT [45–48]. Taking the Cx26 hemichannel as an example, the first N-terminal charged amino acid residue, Asp2, determines the gating polarity in that it closes when the cytoplasmic side becomes positive whereas the D2R and D2K mutants close when the inside potential is negative [45].

Closure of Vj-gating is currently thought to be initiated by the inward movement of a Vj-sensor positioned in the NT (Fig. 2(A)) [45,46,48]. A simple deflection of the NT toward the cytoplasm would contribute to the channel opening as the pore funnel would have more space in the vestibule. In the plug-gating model, an inside-positive Vj initiates the displacement of the Asp2 of Cx26 from the pore vestibule, leading to a collapse of the circular girdle of hydrogen bonds, which results in the assembly of NTs [33]. Because the plug formation may be due to the introduction of the M34A point mutation as described above, it remains to be determined whether the NTs of wild-type Cx26 can form assemblies when Vj is applied or the circular hydrogen bond network through Asp2–Trp5 is broken. For Cx32 channels, Vj-gating polarity is sensitive to a substitution of the residue not only at the second position [46], but also at several positions in the N-terminal residues and at the TM1/EL1 border [45,49,50] as similarly seen in other connexins [51]. Moreover, the homomeric T8D and N2E + G5K hemichannels of Cx32 chimera in which the EL1 of Cx32 is replaced with the EL1 of Cx43 (Cx32*Cx43E1) exhibit a bipolar Vj gating property [46,48], which is inconsistent with the notion that the gating polarity is determined by the relative orientation of a charge dipole in the NT [46]. The simple model that the NTs, perhaps forming a plug, swing inward or outward of the vestibule is insufficient to straightforwardly account for these complicated findings regarding Vj-gating properties.

An intriguing finding is that the heteromeric hemichannels containing a single N2E subunit of Cx32*Cx43E1 can assume subconducting states at positive potentials, leading to an interpretation that the movement of the N-terminal voltage sensor in a single connexin subunit is sufficient to initiate Vj gating [47]. This rearrangement, termed an individual subunit model (Fig. 2(B)), depicts the individual movement of the six subunits in a hemichannel to assume the conformational change, rather than concerted movement by subunit rotation [19], and therefore suggests that hexameric hemichannels or dodecameric junction channels do not need to maintain a sixfold symmetry during the Vj-gating cycle. It has long been taken for granted that the sixfold symmetry can be applied for the structural analysis of vertebrate gap junction channels composed of dodecameric connexin subunits. Asymmetric configurations of constituent subunits are, however, implicated by EM studies of Cx26M34A in which the 2D crystals are formed in an orthorhombic lattice [28]. The plug-gating model also favors the idea of individual subunit movement rather than concerted subunit rotation in that the ion permeation pathway can be created by the movement of just one N-terminal helix of the subunit (Fig. 1(E)).

5. Loop gating

Loop-gating (slow-gating) is an alternative gating property in response to Vj in which a fully closed state is achieved in combination with a series of transient subconducting states and the gating transitions are characterized by slow transition times (~10 ms) [44]. This gating signature is often studied with hemichannels, but is also observed in intercellular junction channels [44,52–54]. While it is suggested that conformational changes in the ELs might be involved in this gating [43], the molecular components as well as the location of the putative gate remain unknown. It was recently demonstrated that loop-gating involves a permeability barrier formed by narrowing the channel pore of the TM1/EL1 domain (Fig. 2(A)) [55,56], and a model of narrowing of the intracellular entrance to the channel pore has been postulated based on the fact that at least four A43C subunits of Cx32*Cx43E1 are required to produce the high-affinity Cd^{2+} binding that locks the channel in the loop-gated closed state [56–58]. The two ELs in the Cx26 X-ray structure provide essential hydrogen bond interactions between apposed hemichannels, and EL2 in particular is critical for the docking specificity when forming a heterotypic junction channel [59–62], making it less likely that loop-gating causes drastic conformational changes in EL interactions. It remains unclear from the current structures if this narrowing of the TM1/EL1 domain can achieve fully occluded ion conduction of the loop-gated state without utilizing both ELs. A high-resolution structure of unopposed hemichannels would help to clarify the conformational rearrangement of extracellular domains.

6. Particle-receptor model

Delmar et al. clearly demonstrated that the CT region of Cx43 is associated with closure at a low pH based on findings that the truncation of CT of Cx43 prevents acidification-induced uncoupling, which is rescued by the co-expression of a truncated CT region as a separate fragment [63,64]. These authors proposed a particle-receptor model with a concept similar to that of the ball-and-chain model originally suggested for voltage-gated ion channels [65,66], that is, CT of Cx43 forms a gating particle and binds in a pH-dependent manner to the cytoplasmic region, specifically the second half of the cytoplasmic loop (Cx43L2) (Fig. 2(A)) [67]. This hypothesis is also applicable to Cx40 [68]. The complicated issue here is that Cx26 and CT-truncated Cx45, which do not possess the CT region corresponding to the gating particle of Cx43 or Cx40, still exhibit pH sensitivity induced by CO_2 acidification, suggesting that the intrinsic mechanisms of pH regulation vary among connexins [68]. Studies using reconstituted Cx32 and Cx32/Cx26 hemichannels showed that the pH effect is modulated by and dependent on pH buffers of amino sulfonate groups, such as MES, HEPES, TAPS, and taurine [69]. While these results cannot simply be combined as they utilize different evaluation systems for pH gating, a similar mechanism has been postulated in which amino sulfonate binds to a cytoplasmic receptor domain independently or by forming a complex between the elements of protonated aminosulfonate, competent CT, and receptor (Fig. 2(A)) [69].

Unfortunately, neither recent EM nor X-ray structures of Cx26 show the disordered CT and CL that are the basis of particle-receptor model. The solution structure of Cx43 CL and CT peptides has been studied by NMR. Cx43L2 includes a short flexible random coil

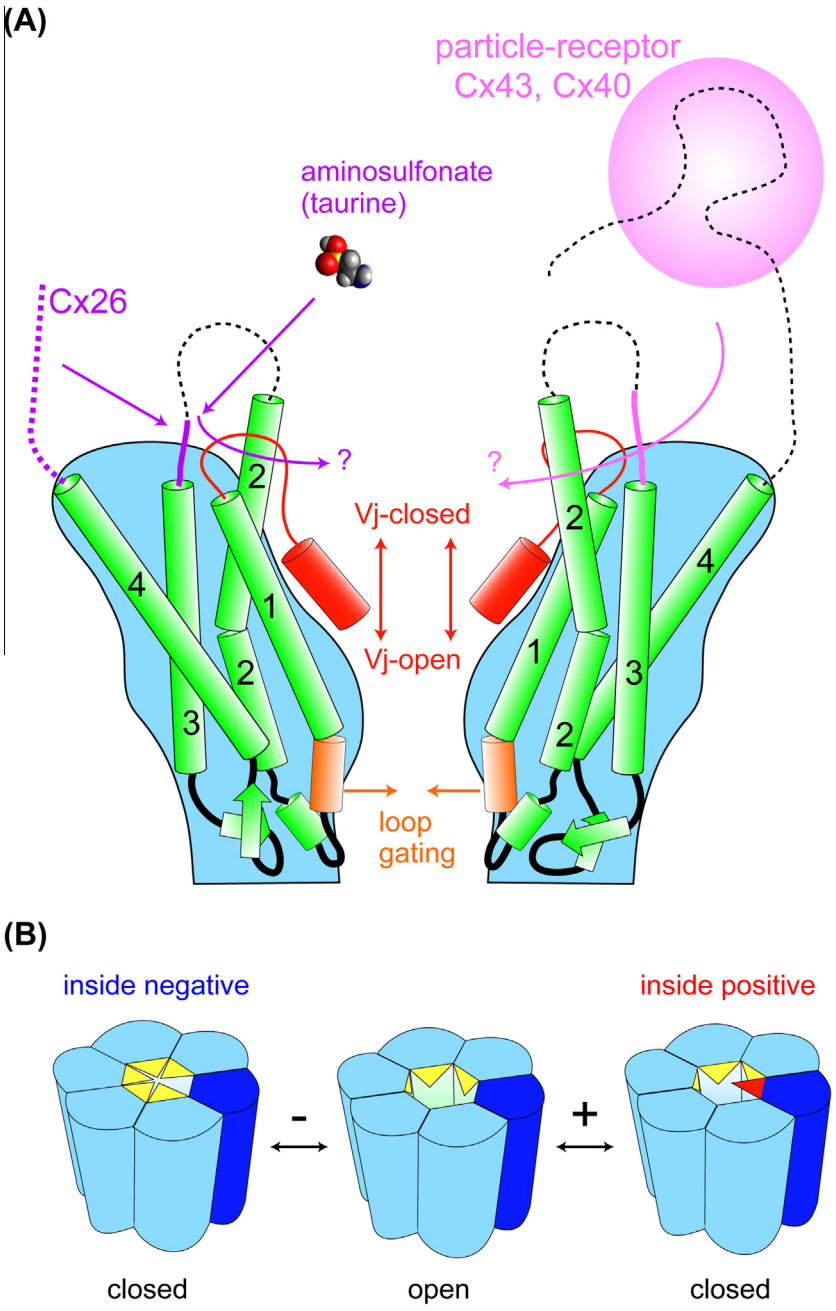

Fig. 2. Gating properties for connexin gap junction channels demonstrated by functional studies. (A) Several types of hypothesized movements for gap junction gating are represented in a model of a hemichannel. It is proposed that Vj-gating (red) is initiated by the inward translocation of charges in the N-terminus that essentially functions as a Vj-sensor [48]. Loop gating (orange) may involve the TM1/EL1 border as the permeability barrier formed by narrowing the channel pore of the TM1/EL1 domain [57]. Particle-receptor model (pink) proposed for Cx43 and Cx40 junction channels, which involves an interaction between the CT ball and the second half of CL (L2 region) as a receptor [67]. Amino sulfonate, taurine here as a representative, binds to Cx26L2, and the short CT of Cx26 is also involved in the intramolecular gating (purple) [74]. (B) Individual subunit model for a Cx32*Cx43E1 hemichannel containing a single N2E mutant subunit [47]. Subunits in a hemichannel are colored in cyan for Cx32*Cx43E1 and in blue for the N2E mutant. N-terminal voltage sensors are drawn as triangles, in yellow for Cx32*Cx43E1, and in red for N2E. Each subunit can respond individually to changes in the polarity of the electric field. Subconducting states can be initiated by the conformational change of one N2E mutant subunit in response to inside positive potential (right). In the case of inside negative potential, the five Cx32*Cx43E1 subunits prefer the conformational change of the voltage sensor resulting in a subconducting state (left).

flanked by two alpha helical regions [70], and the counterpart CT peptide thought to be a binding partner [71] also has two alpha helical domains with a slightly longer connecting loop [72,73]. These domains can alter the conformation depending on the pH induced by acidification, suggesting that these domains have high flexibility [70]. A recent NMR study showed that taurine binds to the CL, not the CT, and that the CT and CL directly interact, suggesting that amino sulfonate modulates CL–CT interactions [74], but the EM structure of Cx26M34A in MES, which has a pH of 5.8, did not show the rigid density of those domains [27,28]. Important observations here are that various sizes of deletion or alanine substitutions in the N-terminal residues of Cx37 induce a defect in intercellular transfer [75], consistent with the decreased junctional permeability and loss of electrical coupling of an N-terminal deletion mutant, Cx26del2-7 [28]. A recent study showed that all oculodentodigital dysplasia-linked N-terminal Cx43 mutants can traffic to the cell surface normally, but the assembled junction-like structures are non-functional [36]. These studies indicate an

alternative mechanism for channel closure when NTs are lost or destabilized. Interestingly, the transition between the full channel closure and an open state mediated by various chemical modulators closely resembles that induced by loop-gating, suggesting similar or shared molecular mechanisms for closure [17]. The CT is also involved in Vj-gating of Cx43 and Cx40 [76–79]. Despite the lack of strong evidence that NTs directly interact with CL or CT, or with the TM1/EL1 border, it is possible that the C-terminal gating particle contributes to the pore entrance along with the cytoplasmic receptor domain, resulting in the modulation of NTs if it blocks the channel pore [67]. Structural studies in which the flexible CL and CT are fixed to reach high resolution are important to gain a better understanding of the gating mechanisms in unresolved cytoplasmic domains that underlie the chemical modulations in conjunction with Vj-gating.

7. Observation by molecular dynamics calculations

Recent molecular dynamics (MD) simulations showed an equilibrated Cx26 structure with a larger minimal pore diameter, which decreased the height of the permeation barrier formed by the NT [80]. In the equilibrated structure, the packing of all four TM helices of each connexin monomer is relaxed, resulting in an increase in the outer diameter of the channel, similar to the rearrangement observed between the X-ray and EM structures of Cx26 [28]. The interpretation is that the average equilibrated structure more closely represents the open Cx26 hemichannel structure than does the crystal structure [57,80]. It should be noted, however, that the MD simulations are based on a modeled Cx26 hemichannel as the initial structure (referred to as "completed structure"), including the Met1 residues in accordance with the NMR solution structure of the N-terminal Cx26 peptide [34], CL and CT based on linear incorporation and extension, and a hemichannel portion being cut out from the X-ray Cx26 gap junction channel. The MD simulations are therefore based on the postulation that the initial model of the Cx26 hemichannel is appropriate, while no hemichannel structure including an intact amino acid sequence has been resolved for any connexin at high resolution.

Considering the electron density map around the NTs of the Cx26 X-ray structure, there is no reason to assume an interpretation other than its being in an open state because a pore diameter over 10 Å can be clearly observed [32]. The possibility of some ambiguity remains, however, in the assignment of the flexible N-terminal residues in the Cx26 X-ray structure. NMR studies of NTs of various connexins further suggest that the conformations at the N-terminal end vary among different connexin isoforms, although the helical structure is likely common [34–36]. Intriguingly, the Cx43G2V mutant, in which the circular hydrogen bond formation seen in the Cx26 X-ray structure might be prevented by additional hydrophobic interactions with Trp4 (corresponding to Trp3 in Cx26), has a non-functional channel [36], indicating that disruption of the key hydrogen bonds results in channel closure while a similar disruption is observed in the average equilibrated structure of the MD calculation [80]. As described above, most functional data with the N-terminal deletion mutants or point mutants, if not all, demonstrate deficient or extremely decreased activity of junction channels or hemichannels [28,35,36,75]. These findings suggest that the appropriate N-terminal arrangement is essential for normal channel function. To resolve the discrepancies surrounding these issues, structural studies are required to elucidate the contribution of the unresolved cytoplasmic domains and MD simulations are needed to expand the time scale of the transition between the open and closed configurations, probably on the millisecond order, based on empirically determined structures.

8. Outlook

The plug-gating model has been proposed for Cx26 as a possible mechanism for gap junction channels to account for the alternative rearrangement of conformations in a closed state by forming a physical blockage with the NTs in the pore of each hemichannel. In this model, a junction channel is permeable only when both hemichannels assume the open conformation, although it is uncertain whether the plug-gated state represents a physiologic gating mechanism in connexin gap junction channels. Given the pore funnel configuration in the Cx26 X-ray structure, it is no wonder that modulations of ELs, CL, and CT of connexin peptides involved in the gating properties described above would function in coordination with the N-terminal rearrangement. It is also unlikely that a wide pore over 10 Å in diameter can be closed to be non-conductive by just a partial conformational change, such as a twist or narrowing of a certain helix, without some sort of physical blockage of the pore pathway. The X-ray structure of Cx26 crystallized in 3D without Ca^{2+} reveals an arrangement very similar to that of transmembrane helices in the EM structure where Ca^{2+} was added during 2D crystallization. Recent 3D structures of connexin gap junction channels do not show a drastic conformational change of transmembrane domains, such as tilting in the rotation model [19]. On the other hand, Met34, mutated in the Cx26 EM structure, is not a highly conserved residue in the connexin family as Leu or Val appears in some other connexins, raising questions about how the N-terminal arrangement, such as the pore funnel in the Cx26 X-ray structure, is conserved and whether it is common in the connexin family. One structure alone cannot satisfactorily explain all the gating properties implicated by functional studies. The connexin structures currently available do not clearly, readily, and consistently account for these properties. More connexin structures need to be observed in a closed state, preferably at high resolution, to provide better insight into the physiologic gating mechanism of connexin gap junction channels. For chemical gating, connexin channels could be crystallized with chemical modulators. A critical issue, however, is how to fix the flexible cytoplasmic domains in a stable position. A view of the Vj-gated conformation might be difficult to obtain because of the impracticality of applying Vj in general crystallization conditions. Structural analyses of connexin mutants with an active function specifically favoring the subconducting state may provide some insight. Knowledge of the structure of connexin hemichannels would be useful to elucidate the potentially different extracellular conformations between the docked and undocked forms, and in association with loop-gating. The challenge here is determining how to isolate, purify, and crystallize connexin hemichannels that are not in junction form. Studies of the gating mechanisms of gap junction channels must correlate structure with function based on high-resolution models. Observations of more "closed" structures demonstrating the cytoplasmic domains at high resolution will contribute to a better understanding of this relationship and the biologic significance of the complicated closure mechanisms of connexin channels *in vivo*.

Acknowledgments

I am grateful to Yoshinori Fujiyoshi for critical discussion. This work was supported by the Japan New Energy and Industrial Technology Development Organization (NEDO); and the Platform for Drug Design, Discovery, and Development from the Ministry of Education, Culture, Sports, Science, and Technology (MEXT), Japan.

References

[1] Gilula, N.B. (1978) in: Intercellular Junctions and Synapses (Feldman, J., Gilula, N.B. and Pitts, J.D., Eds.), pp. 1–22, Chapman & Hall, London.
[2] Paul, D.L. (1986) Molecular cloning of cDNA for rat liver gap junction protein. J. Cell Biol. 103, 123–134.
[3] Kumar, N.M. and Gilula, N.B. (1986) Cloning and characterization of human and rat liver cDNAs coding for a gap junction protein. J. Cell Biol. 103, 767–776.
[4] Beyer, E.C., Paul, D.L. and Goodenough, D.A. (1987) Connexin43: a protein from rat heart homologous to a gap junction protein from liver. J. Cell Biol. 105, 2621–2629.
[5] Scemes, E., Spray, D.C. and Meda, P. (2009) Connexins, pannexins, innexins: novel roles of "hemi-channels". Pflugers Arch. 457, 1207–1226.
[6] Goodenough, D.A. and Gilula, N.B. (1974) The splitting of hepatocyte gap junctions and zonulae occludentes with hypertonic disaccharides. J. Cell Biol. 61, 575–590.
[7] Zampighi, G. and Unwin, P.N. (1979) Two forms of isolated gap junctions. J. Mol. Biol. 135, 451–464.
[8] Henderson, D., Eibl, H. and Weber, K. (1979) Structure and biochemistry of mouse hepatic gap junctions. J. Mol. Biol. 132, 193–218.
[9] Hertzberg, E.L. and Gilula, N.B. (1979) Isolation and characterization of gap junctions from rat liver. J. Biol. Chem. 254, 2138–2147.
[10] Fallon, R.F. and Goodenough, D.A. (1981) Five-hour half-life of mouse liver gap-junction protein. J. Cell Biol. 90, 521–526.
[11] Makowski, L., Caspar, D.L., Phillips, W.C. and Goodenough, D.A. (1977) Gap junction structures. II. Analysis of the X-ray diffraction data. J. Cell Biol. 74, 629–645.
[12] Turin, L. and Warner, A. (1977) Carbon dioxide reversibly abolishes ionic communication between cells of early amphibian embryo. Nature 270, 56–57.
[13] Rose, B., Simpson, I. and Loewenstein, W.R. (1977) Calcium ion produces graded changes in permeability of membrane channels in cell junction. Nature 267, 625–627.
[14] Spray, D.C., Harris, A.L. and Bennett, M.V.L. (1981) Gap junctional conductance is a simple and sensitive function of intracellular pH. Science 211, 712–715.
[15] Spray, D.C., Harris, A.L. and Bennett, M.V. (1979) Voltage dependence of junctional conductance in early amphibian embryos. Science 204, 432–434.
[16] Harris, A.L., Spray, D.C. and Bennett, M.V. (1981) Kinetic properties of a voltage-dependent junctional conductance. J. Gen. Physiol. 77, 95–117.
[17] Harris, A.L. (2001) Emerging issues of connexin channels: biophysics fills the gap. Q. Rev. Biophys. 34, 325–472.
[18] Unwin, P.N. and Zampighi, G. (1980) Structure of the junction between communicating cells. Nature 283, 545–549.
[19] Unwin, P.N. and Ennis, P.D. (1984) Two configurations of a channel-forming membrane protein. Nature 307, 609–613.
[20] Unwin, P.N. and Ennis, P.D. (1983) Calcium-mediated changes in gap junction structure: evidence from the low angle X-ray pattern. J. Cell Biol. 97, 1459–1466.
[21] Unwin, N. (1989) The structure of ion channels in membranes of excitable cells. Neuron 3, 665–676.
[22] Perkins, G., Goodenough, D. and Sosinsky, G. (1997) Three-dimensional structure of the gap junction connexon. Biophys. J. 72, 533–544.
[23] Kumar, N.M., Friend, D.S. and Gilula, N.B. (1995) Synthesis and assembly of human beta 1 gap junctions in BHK cells by DNA transfection with the human beta 1 cDNA. J. Cell Sci. 108, 3725–3734.
[24] Unger, V.M., Kumar, N.M., Gilula, N.B. and Yeager, M. (1999) Expression, two-dimensional crystallization, and electron cryo-crystallography of recombinant gap junction membrane channels. J. Struct. Biol. 128, 98–105.
[25] Unger, V.M., Kumar, N.M., Gilula, N.B. and Yeager, M. (1999) Three-dimensional structure of a recombinant gap junction membrane channel. Science 283, 1176–1180.
[26] Guan, X., Cravatt, B.F., Ehring, G.R., Hall, J.E., Boger, D.L., Lerner, R.A. and Gilula, N.B. (1997) The sleep-inducing lipid oleamide deconvolutes gap junction communication and calcium wave transmission in glial cells. J. Cell Biol. 139, 1785–1792.
[27] Oshima, A., Tani, K., Hiroaki, Y., Fujiyoshi, Y. and Sosinsky, G.E. (2007) Three-dimensional structure of a human connexin26 gap junction channel reveals a plug in the vestibule. Proc. Natl. Acad. Sci. USA 104, 10034–10039.
[28] Oshima, A., Tani, K., Toloue, M.M., Hiroaki, Y., Smock, A., Inukai, S., Cone, A., Nicholson, B.J., Sosinsky, G.E. and Fujiyoshi, Y. (2011) Asymmetric configurations and N-terminal rearrangements in connexin26 gap junction channels. J. Mol. Biol. 405, 724–735.
[29] Kelsell, D.P., Dunlop, J., Stevens, H.P., Lench, N.J., Liang, J.N., Parry, G., Mueller, R.F. and Leigh, I.M. (1997) Connexin26 mutations in hereditary non-syndromic sensorineural deafness. Nature 387, 80–83.
[30] Oshima, A., Doi, T., Mitsuoka, K., Maeda, S. and Fujiyoshi, Y. (2003) Roles of Met-34, Cys-64, and Arg-75 in the assembly of human connexin26. Implication for key amino acid residues for channel formation and function. J. Biol. Chem. 278, 1807–1816.
[31] Oshima, A., Tani, K., Hiroaki, Y., Fujiyoshi, Y. and Sosinsky, G.E. (2008) Projection structure of a N-terminal deletion mutant of connexin26 channel with decreased central pore density. Cell Commun. Adhes. 15, 85–93.
[32] Maeda, S., Nakagawa, S., Suga, M., Yamashita, E., Oshima, A., Fujiyoshi, Y. and Tsukihara, T. (2009) Structure of the connexin26 gap junction channel at 3.5 Å resolution. Nature 458, 597–602.
[33] Maeda, S. and Tsukihara, T. (2011) Structure of the gap junction channel and its implications for its biological functions. Cell. Mol. Life Sci. 68, 1115–1129.
[34] Purnick, P.E., Benjamin, D.C., Verselis, V.K., Bargiello, T.A. and Dowd, T.L. (2000) Structure of the amino terminus of a gap junction protein. Arch. Biochem. Biophys. 381, 181–190.
[35] Kyle, J.W., Berthoud, V.M., Kurutz, J., Minogue, P.J., Greenspan, M., Hanck, D.A. and Beyer, E.C. (2009) The N terminus of connexin37 contains an alpha-helix that is required for channel function. J. Biol. Chem. 284, 20418–20427.
[36] Shao, Q., Liu, Q., Lorentz, R., Gong, X.Q., Bai, D., Shaw, G.S. and Laird, D.W. (2012) Structure and functional studies of N-terminal Cx43 mutants linked to oculodentodigital dysplasia. Mol. Biol. Cell 23, 3312–3321.
[37] Perkins, G.A., Goodenough, D.A. and Sosinsky, G.E. (1998) Formation of the gap junction intercellular channel requires a 30° rotation for interdigitating two apposing connexons. J. Mol. Biol. 277, 171–177.
[38] Fleishman, S.J., Unger, V.M., Yeager, M. and Ben-Tal, N. (2004) A Calpha model for the transmembrane alpha helices of gap junction intercellular channels. Mol. Cell 15, 879–888.
[39] Müller, D.J., Hand, G.M., Engel, A. and Sosinsky, G.E. (2002) Conformational changes in surface structures of isolated connexin26 gap junctions. EMBO J. 21, 3598–3607.
[40] Thimm, J., Mechler, A., Lin, H., Rhee, S. and Lal, R. (2005) Calcium-dependent open/closed conformations and interfacial energy maps of reconstituted hemichannels. J. Biol. Chem. 280, 10646–10654.
[41] Gaßmann, O., Kreir, M., Ambrosi, C., Pranskevich, J., Oshima, A., Röling, C., Sosinsky, G., Fertig, N. and Steinem, C. (2009) The M34A mutant of Connexin26 reveals active conductance states in pore-suspending membranes. J. Struct. Biol. 168, 168–176.
[42] Moreno, A.P., Rook, M.B., Fishman, G.I. and Spray, D.C. (1994) Gap junction channels: distinct voltage-sensitive and -insensitive conductance states. Biophys. J. 67, 113–119.
[43] Trexler, E.B., Bennett, M.V., Bargiello, T.A. and Verselis, V.K. (1996) Voltage gating and permeation in a gap junction hemichannel. Proc. Natl. Acad. Sci. USA 93, 5836–5841.
[44] Bukauskas, F.F. and Verselis, V.K. (2004) Gap junction channel gating. Biochim. Biophys. Acta 1662, 42–60.
[45] Verselis, V.K., Ginter, C.S. and Bargiello, T.A. (1994) Opposite voltage gating polarities of two closely related connexins. Nature 368, 348–351.
[46] Purnick, P.E., Oh, S., Abrams, C.K., Verselis, V.K. and Bargiello, T.A. (2000) Reversal of the gating polarity of gap junctions by negative charge substitutions in the N-terminus of connexin32. Biophys. J. 79, 2403–2415.
[47] Oh, S., Abrams, C.K., Verselis, V.K. and Bargiello, T.A. (2000) Stoichiometry of transjunctional voltage-gating polarity reversal by a negative charge substitution in the amino terminus of a connexin32 chimera. J. Gen. Physiol. 116, 13–31.
[48] Oh, S., Rivkin, S., Tang, Q., Verselis, V.K. and Bargiello, T.A. (2004) Determinants of gating polarity of a connexin32 hemichannel. Biophys. J. 87, 912–928.
[49] Rubin, J.B., Verselis, V.K., Bennett, M.V. and Bargiello, T.A. (1992) Molecular analysis of voltage dependence of heterotypic gap junctions formed by connexins 26 and 32. Biophys. J. 62, 183–193.
[50] Oh, S., Rubin, J.B., Bennett, M.V., Verselis, V.K. and Bargiello, T.A. (1999) Molecular determinants of electrical rectification of single channel conductance in gap junctions formed by connexins 26 and 32. J. Gen. Physiol. 114, 339–364.
[51] Tong, J.J. and Ebihara, L. (2006) Structural determinants for the differences in voltage gating of chicken Cx56 and Cx45.6 gap-junctional hemichannels. Biophys. J. 91, 2142–2154.
[52] Oh, S., Ri, Y., Bennett, M.V., Trexler, E.B., Verselis, V.K. and Bargiello, T.A. (1997) Changes in permeability caused by connexin32 mutations underlie X-linked Charcot-Marie-Tooth disease. Neuron 19, 927–938.
[53] Bukauskas, F.F., Angele, A.B., Verselis, V.K. and Bennett, M.V. (2002) Coupling asymmetry of heterotypic connexin45/connexin43-EGFP gap junctions: properties of fast and slow gating mechanisms. Proc. Natl. Acad. Sci. USA 99, 7113–7118.
[54] Rackauskas, M., Kreuzberg, M.M., Pranevicius, M., Willecke, K., Verselis, V.K. and Bukauskas, F.F. (2007) Gating properties of heterotypic gap junction channels formed of connexins 40, 43, and 45. Biophys. J. 92, 1952–1965.
[55] Verselis, V.K., Trelles, M.P., Rubinos, C., Bargiello, T.A. and Srinivas, M. (2009) Loop gating of connexin hemichannels involves movement of pore-lining residues in the first extracellular loop domain. J. Biol. Chem. 284, 4484–4493.
[56] Tang, Q., Dowd, T.L., Verselis, V.K. and Bargiello, T.A. (2009) Conformational changes in a pore-forming region underlie voltage-dependent "loop gating" of an unopposed connexin hemichannel. J. Gen. Physiol. 133, 555–570.
[57] Bargiello, T.A., Tang, Q., Oh, S. and Kwon, T. (2012) Voltage-dependent conformational changes in connexin channels. Biochim. Biophys. Acta 1818, 1807–1822.
[58] Kwon, T., Tang, Q. and Bargiello, T.A. (2013) Voltage-dependent gating of the Cx32*43E1 hemichannel: conformational changes at the channel entrances. J. Gen. Physiol. 141, 243–259.
[59] White, T.W., Bruzzone, R., Wolfram, S., Paul, D.L. and Goodenough, D.A. (1994) Selective interactions among the multiple connexin proteins expressed in the vertebrate lens: the second extracellular domain is a determinant of compatibility between connexins. J. Cell Biol. 125, 879–892.
[60] Bruzzone, R., White, T.W. and Paul, D.L. (1994) Expression of chimeric connexins reveals new properties of the formation and gating behavior of gap junction channels. J. Cell Sci. 107, 955–967.

[61] Nakagawa, S., Maeda, S. and Tsukihara, T. (2010) Structural and functional studies of gap junction channels. Curr. Opin. Struct. Biol. 20, 423–430.
[62] Nakagawa, S., Gong, X.Q., Maeda, S., Dong, Y., Misumi, Y., Tsukihara, T. and Bai, D. (2011) Asparagine 175 of connexin32 is a critical residue for docking and forming functional heterotypic gap junction channels with connexin26. J. Biol. Chem. 286, 19672–19681.
[63] Liu, S., Taffet, S., Stoner, L., Delmar, M., Vallano, M.L. and Jalife, J. (1993) A structural basis for the unequal sensitivity of the major cardiac and liver gap junctions to intracellular acidification: the carboxyl tail length. Biophys. J. 64, 1422–1433.
[64] Morley, G.E., Taffet, S.M. and Delmar, M. (1996) Intramolecular interactions mediate pH regulation of connexin43 channels. Biophys. J. 70, 1294–1302.
[65] Armstrong, C.M. and Bezanilla, F. (1977) Inactivation of the sodium channel. II. Gating current experiments. J. Gen. Physiol. 70, 567–590.
[66] Hoshi, T., Zagotta, W.N. and Aldrich, R.W. (1990) Biophysical and molecular mechanisms of Shaker potassium channel inactivation. Science 250, 533–538.
[67] Delmar, M., Coombs, W., Sorgen, P., Duffy, H.S. and Taffet, S.M. (2004) Structural bases for the chemical regulation of Connexin43 channels. Cardiovasc. Res. 62, 268–275.
[68] Stergiopoulos, K., Alvarado, J.L., Mastroianni, M., Ek-Vitorin, J.F., Taffet, S.M. and Delmar, M. (1999) Hetero-domain interactions as a mechanism for the regulation of connexin channels. Circ. Res. 84, 1144–1155.
[69] Bevans, C.G. and Harris, A.L. (1999) Regulation of connexin channels by pH. Direct action of the protonated form of taurine and other aminosulfonates. J. Biol. Chem. 274, 3711–3719.
[70] Duffy, H.S., Sorgen, P.L., Girvin, M.E., O'Donnell, P., Coombs, W., Taffet, S.M., Delmar, M. and Spray, D.C. (2002) PH-dependent intramolecular binding and structure involving Cx43 cytoplasmic domains. J. Biol. Chem. 277, 36706–36714.
[71] Duffy, H.S., Delmar, M., Coombs, W., Taffet, S.M., Hertzberg, E.L. and Spray, D.C. (2001) Functional demonstration of connexin-protein binding using surface plasmon resonance. Cell Commun. Adhes. 8, 225–229.
[72] Sorgen, P.L., Duffy, H.S., Cahill, S.M., Coombs, W., Spray, D.C., Delmar, M. and Girvin, M.E. (2002) Sequence-specific resonance assignment of the carboxyl terminal domain of Connexin43. J. Biomol. NMR 23, 245–246.
[73] Sorgen, P.L., Duffy, H.S., Sahoo, P., Coombs, W., Delmar, M. and Spray, D.C. (2004) Structural changes in the carboxyl terminus of the gap junction protein connexin43 indicates signaling between binding domains for c-Src and zonula occludens-1. J. Biol. Chem. 279, 54695–54701.
[74] Locke, D., Kieken, F., Tao, L., Sorgen, P.L. and Harris, A.L. (2011) Mechanism for modulation of gating of connexin26-containing channels by taurine. J. Gen. Physiol. 138, 321–339.
[75] Kyle, J.W., Minogue, P.J., Thomas, B.C., Domowicz, D.A., Berthoud, V.M., Hanck, D.A. and Beyer, E.C. (2008) An intact connexin N-terminus is required for function but not gap junction formation. J. Cell Sci. 121, 2744–2750.
[76] Revilla, A., Castro, C. and Barrio, L.C. (1999) Molecular dissection of transjunctional voltage dependence in the connexin-32 and connexin-43 junctions. Biophys. J. 77, 1374–1383.
[77] Anumonwo, J.M., Taffet, S.M., Gu, H., Chanson, M., Moreno, A.P. and Delmar, M. (2001) The carboxyl terminal domain regulates the unitary conductance and voltage dependence of connexin40 gap junction channels. Circ. Res. 88, 666–673.
[78] Moreno, A.P., Chanson, M., Elenes, S., Anumonwo, J., Scerri, I., Gu, H., Taffet, S.M. and Delmar, M. (2002) Role of the carboxyl terminal of connexin43 in transjunctional fast voltage gating. Circ. Res. 90, 450–457.
[79] González, D., Gómez-Hernández, J.M. and Barrio, L.C. (2007) Molecular basis of voltage dependence of connexin channels: an integrative appraisal. Prog. Biophys. Mol. Biol. 94, 66–106.
[80] Kwon, T., Harris, A.L., Rossi, A. and Bargiello, T.A. (2011) Molecular dynamics simulations of the Cx26 hemichannel: evaluation of structural models with Brownian dynamics. J. Gen. Physiol. 138, 475–493.